Nov 5th, 12:00 AM - 12:00 AM

Constrained Finite Element Method: Demonstrative Examples on the Global Modes of Thin-Walled Members

S. Ádány

Twenty-Second International Specialty Conference on Cold-Formed Steel Structures
St. Louis, Missouri, USA, November 5 & 6, 2014

Constrained finite element method: demonstrative examples on the global modes of thin-walled members

S. Ádány[1]

Abstract

In this paper a novel method is presented for the modal decomposition of thin-walled members. The proposed method follows the logic of the constrained finite strip method (cFSM), however, polynomial longitudinal shape functions are applied together with a longitudinal discretization. Thus, strips are transformed into multiple shell finite elements. The longitudinal shape functions are selected in such a way that modal decomposition similar to cFSM can be realized, therefore, the new method can conveniently be described as constrained finite element method (cFEM), possessing all the modal features of cFSM, but with significantly more flexible applicability. The method is briefly presented and illustrated by global buckling problems.

Introduction

For thin-walled members subjected to compressive axial stresses three types of basic buckling phenomena are usually distinguished: local, distortional and global buckling. Each has its characteristic post-buckling behavior, thus, it is important to clearly classify the various buckling modes in order to be able to assess realistic design capacity.

Two basic tasks can be mentioned in the context of global-distortional-local classification. One is the pure critical load calculation when the aim is to calculate critical load with forcing the member to deform in accordance with a buckling class. The other is buckling mode identification, when critical load is calculated without any preliminary restriction on the deformations, and then the buckled shape it is identified, i.e., the contributions of various mode classes are defined. To be able to solve both of these basic tasks, the solution method must use a modal base system, i.e., the full displacement field of the member must be expressed by special modal base functions. During the last few decades two approaches have been evolved possessing the above modal feature. First, the generalized beam theory (GBT), see Silvestre et al (2011), later the constrained

[1] Associate Professor, Budapest University of Technology and Economics, Budapest, Hungary

finite strip method (cFSM), see Adany and Schafer (2008). Both approaches have limitations. For example, in case of cFSM the member and its loading have to be uniform along the member length as a direct consequence of the initial assumptions of the semianalytical FSM (Cheung and Tham, 1997).

To overcome the limitations of FSM, a novel shell finite element is proposed here. The longitudinal shape functions are selected in such a way that constraining similar to cFSM can be realized. The resulted method can readily be described as constrained finite element method (cFEM) which has the same advantageous features as those of the original cFSM, while provides more general practical applicability.

In this paper the proposed cFEM method is briefly presented, then numerical examples are shown. The numerical results prove the concept of the new method, as well as demonstrate its potential. Though the method itself is general, in this paper only global buckling problems are shown, while other buckling types will be discussed in other papers.

From FSM to FEM

In finite strip method a member is discretized into longitudinal strips, instead of finite element method, which applies discretization in both the longitudinal and transverse directions. In Figure 1 a single strip is highlighted, along with the local coordinate system and the degrees of freedom (DOF) for the strip.

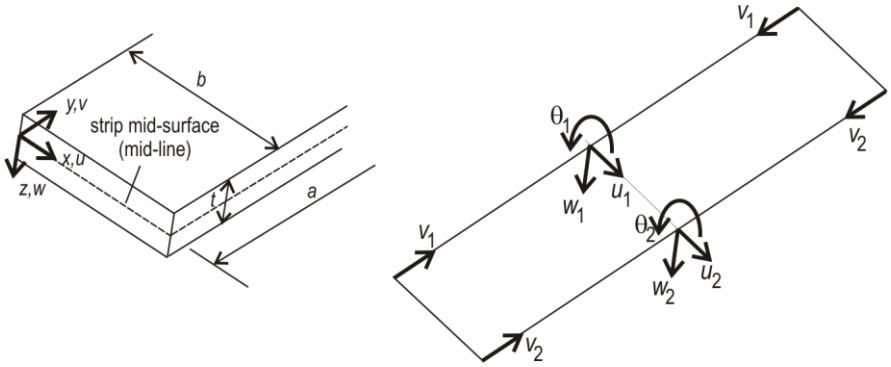

Figure 1: Coordinates, Finite Strip DOF

In FSM the displacements are approximated as follows.

$$u(x,y) = \begin{bmatrix} N_{x1,1} & N_{x1,2} \end{bmatrix} \begin{bmatrix} u_1 \\ u_2 \end{bmatrix} \sin\frac{m\pi y}{a} \tag{1}$$

$$v(x,y) = \begin{bmatrix} N_{x1,1} & N_{x1,2} \end{bmatrix} \begin{bmatrix} v_1 \\ v_2 \end{bmatrix} \cos\frac{m\pi y}{a} \tag{2}$$

$$w(x,y) = \begin{bmatrix} N_{x3,1} & N_{x3,2} & N_{x3,3} & N_{x3,4} \end{bmatrix} \begin{bmatrix} w_1 \\ \vartheta_1 \\ w_2 \\ \vartheta_2 \end{bmatrix} \sin\frac{m\pi y}{a} \tag{3}$$

with the linear (N_{x1}) and cubic (N_{x3}) transverse shape functions as follows:

$$N_{x1,1} = 1 - \frac{x}{b} \quad \text{and} \quad N_{x1,2} = \frac{x}{b} \tag{4}$$

$$N_{x3,1} = 1 - \frac{3x^2}{b^2} + \frac{2x^3}{b^3} \qquad N_{x3,2} = -x + \frac{2x^2}{b} - \frac{x^3}{b^2}$$

$$N_{x3,3} = \frac{3x^2}{b^2} - \frac{2x^3}{b^3} \qquad N_{x3,4} = \frac{x^2}{b} - \frac{x^3}{b^2} \tag{5}$$

where a is the member length, and b is the strip width.

The above formulae represent pinned-pinned boundary conditions. An important feature of the longitudinal shape functions is that (i) the same longitudinal functions are used for u and w, and (ii) the longitudinal function for v is the first derivative of that used for u and w. By keeping these above characteristics, the formulae can be generalized, and various end conditions can be described, as in Cheung and Tham (1997) and Li and Schafer (2009), where trigonometric series are used.

Here an alternative generalization is applied: instead of using trigonometric functions (or function series), polynomial longitudinal shape functions are used, as typical in finite element method. Our goal here is to find longitudinal shape functions with the following features: (i) for w displacement $C^{(1)}$ continuous functions should be used which are practically useful for handling various end restraint conditions, (ii) shape functions for u are identical to those for w, (iii) they must be able to exactly satisfy the constraining criteria for mode decomposition. Thus, for u and w standard cubic shape functions are used, while second-order functions are used (i.e. 3-point interpolation) for v (which is essential for the constraining). The interpolations are as follows:

$$u(x,y)=\begin{bmatrix}N_{x1,1} & N_{x1,2}\end{bmatrix}\begin{bmatrix}u_1\\u_2\end{bmatrix}\times\begin{bmatrix}N_{y3,1} & N_{y3,2} & N_{y3,3} & N_{y3,4}\end{bmatrix}\begin{bmatrix}c_{u1}\\c_{u2}\\c_{u3}\\c_{u4}\end{bmatrix} \tag{6}$$

$$v(x,y)=\begin{bmatrix}N_{x1,1} & N_{x1,2}\end{bmatrix}\begin{bmatrix}v_1\\v_2\end{bmatrix}\times\begin{bmatrix}N_{y2,1} & N_{y2,2} & N_{y2,3}\end{bmatrix}\begin{bmatrix}c_{v1}\\c_{v2}\\c_{v3}\end{bmatrix} \tag{7}$$

$$w(x,y)=\begin{bmatrix}N_{x3,1} & N_{x3,2} & N_{x3,3} & N_{x3,4}\end{bmatrix}\begin{bmatrix}w_1\\\vartheta_1\\w_2\\\vartheta_2\end{bmatrix}\times\begin{bmatrix}N_{y3,1} & N_{y3,2} & N_{y3,3} & N_{y3,4}\end{bmatrix}\begin{bmatrix}c_{w1}\\c_{w2}\\c_{w3}\\c_{w4}\end{bmatrix} \tag{8}$$

with the second-order (N_{y2}) and third-order (N_{y3}) longitudinal shape functions as:

$$N_{y2,1}=1-\frac{3y}{a}+\frac{2y^2}{a^2}\quad N_{y2,2}=\frac{4y}{a}-\frac{4y^2}{a^2}\quad N_{y2,3}=-\frac{y}{a}+\frac{2y^2}{a^2} \tag{9}$$

$$\begin{aligned}&N_{y3,1}=1-\frac{3y^2}{a^2}+\frac{2y^3}{a^3}\quad N_{y3,2}=-y+\frac{2y^2}{a}-\frac{y^3}{a^2}\\&N_{y3,3}=\frac{3y^2}{a^2}-\frac{2y^3}{a^3}\qquad N_{y3,4}=\frac{y^2}{a}-\frac{y^3}{a^2}\end{aligned} \tag{10}$$

With the above longitudinal shape functions the ‘strip’ is transformed into a ‘shell finite element’. This shell element is unusual, since longitudinal and transverse directions are distinguished, and different interpolation functions are used for the various degrees of freedom and various directions, including linear, second-order and cubic interpolation functions. The details of this shell element are not discussed here, but it can be understood that the resulted shell element has 6 nodes, some with 7- DOF and some with 1-DOF, so that the total number of DOF of the element is 30.

Constraining

In this paper global modes are discussed only. The global modes satisfy three criteria: (i) no transverse extension, (ii) no in-plane shear, and (iii) no transverse curvature. With the proposed shape functions all these three criteria can be exactly satisfied, which is demonstrated as follows.

The ‘no transverse strain’ criterion is:

$$\varepsilon_x = \frac{\partial u}{\partial x} = 0 \tag{11}$$

Using the above shape functions:

$$\begin{bmatrix} -\frac{1}{b} & \frac{1}{b} \end{bmatrix} \begin{bmatrix} u_1 \\ u_2 \end{bmatrix} \times \begin{bmatrix} N_{y3,1} & N_{y3,2} & N_{y3,3} & N_{y3,4} \end{bmatrix} \begin{bmatrix} c_{u1} \\ c_{u2} \\ c_{u3} \\ c_{u4} \end{bmatrix} = 0 \tag{12}$$

This is satisfied for any y if (and only if) $u_1 = u_2$.

The ‘no in-plane shear’ criterion is:

$$\gamma_{xy} = \frac{\partial u}{\partial y} + \frac{\partial v}{\partial x} = 0 \tag{13}$$

Using the above shape functions, performing the derivations and considering also the ‘no transverse strain’ criterion (i.e., $u_1 = u_2 = u$) the criteria lead to a second-order polynomial expression as follows:

$$\gamma_{xy} = \sum_{i=0}^{2} \alpha_i y^i = 0 \tag{14}$$

This is satisfied only if all the α_i coefficients are zero, which leads to a system of 3 equations from which the following relationships are obtained between the DOF of the element:

$$\left.\begin{aligned} c_{v1} \frac{v_2 - v_1}{b} &= u c_{u2} \\ c_{v2} \frac{v_2 - v_1}{b} &= u c \left(\frac{3c_{u1}}{2a} - \frac{c_{u2}}{4} - \frac{3c_{u3}}{2a} - \frac{c_{u4}}{4} \right) \\ c_{v3} \frac{v_2 - v_1}{b} &= u c_{u4} \end{aligned}\right\} \tag{15}$$

It is to note that the right-hand-side of the above equations are the angle of rotation (around z axis) of the edge line of the element at $y = 0$, $y = a/2$, and at $y = a$, respectively, which angles are unambiguously defined by the lateral displacement of the element (and vica-versa).

Finally, the 'no transverse curvature' criterion is as follows:

$$\kappa_{xx} = \frac{\partial^2 w}{\partial x^2} = 0 \tag{16}$$

By substituting the $w(x,y)$ function the transverse curvature expression can be written in the form:

$$\kappa_{xx} = = \sum_{j=0}^{3} \sum_{i=0}^{1} \alpha_{ij} x^i y^j = 0 \tag{17}$$

This is satisfied only if all the α_{ij} coefficients are zero, which lead to a system of equations (in this case: 8 equations). This system of equations leads to 8 relationships between the various nodal displacements, which finally can be written by two equations as follows:

$$\vartheta_1 = \vartheta_2 \text{ and } \frac{w_1 - w_2}{b} = \vartheta_1 \quad (\text{or} \quad = \vartheta_2) \tag{18}$$

Note, these two equations express that the edge of the element at any y location remains straight.

Numerical examples: overview of the considered problems

Both column and beam problems are considered, as shown in Fig 2. In all the cases the member is assumed to have simple supports at both ends. In all the examples buckling is solved, by calculating critical forces or critical moments. In case of columns major- and minor-axis flexural buckling (referred also as 'F maj' and 'F min') and pure torsional buckling (referred also as 'T') are considered, while in case of beams lateral-torsional buckling (LT) is calculated. (Note, here doubly-symmetrical cross-sections are discussed only.) Various buckling lengths are assumed, including (very) short and long members.

Two cross-sections are selected, as shown in Fig 3. The first one is the same IPE400 profile. The one named 'I-narrow' is similar to IPE400, but with substantially narrower flanges.

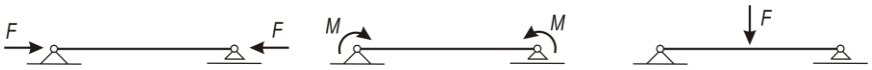

Load1 Load2 Load3

Figure 2: The considered buckling problems

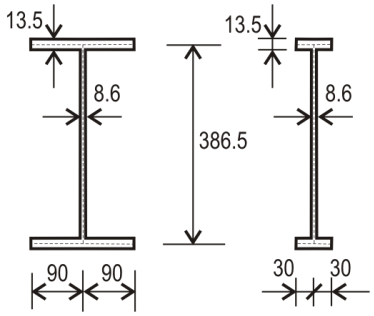

IPE400 I-narrow

Figure 3: Cross-sections for numerical studies (dimensions in mm)

Two materials are considered, both having characteristics similar to regular steel. However, previous studies highlighted that the applied constraining (namely: the 'no transverse strain' criterion) introduces an increase of the axial stiffness (as well as all the stiffnesses associated with warping), therefore, if the comparison of various methods is the goal, the Possion's ratio should be set to zero. (For more details, see Ádány and Visy, 2012). 'Mat0' here is an isotropic material, characterized by E = 210 000 MPa, ν=0, and G = 105 000 MPa. 'Mat1' is an orthotropic material, with E = 210 000 MPa, ν=0, and G = 80 770 MPa (i.e., the shear modulus is equal to that of a real steel material).

Numerical examples: methods

The problems are solved by using various methods. Namely: (i) analytical formulae, (ii) shell finite element analysis by using a commercial software package, (iii) constrained finite strip analysis as implemented in CUFSM (2006) (iv) generalized beam theory as implemented in GBTUL (2008), and (v) the here presented constrained finite element analysis (cFEM).

cFEM analysis

In case of cFEM analysis the member is divided into 10 (equal length) elements longitudinally, while the cross-section is discretized into 12 elements, with four elements in the web and four elements in each flange. This, without the constraints, altogether means 1131 DOF. When constraints are used, the total DOF number drastically reduces and drops to 87. However, if supports are considered and the analysis is limited to a specific buckling mode, the effective DOF number is further decreasing. For example, in case a flexural buckling problem DOF number can be as little as 20 (practically: twice the number of the elements' number longitudinally). Note, the same discretization is used for both cross-sections and for any member length. This leads to varying aspect ratios for the individual finite elements. In the performed numerical studies aspect ratio up to 70 has been applied, which is much higher than normally recommended, however, unlike in typical shell finite element applications, here the integrations are performed exactly, therefore, no numerical problems have been experienced.

The end restraint is also shown in Fig 4. Moreover, a longitudinal support is defined at the very middle node of the member.

In case of loading cases Load1 and Load2 the end force and end moment is defined as a distributed loading over the end cross-section. In case of Load3 the point load is defined as a concentrated force acting on the node in the very middle of the member.

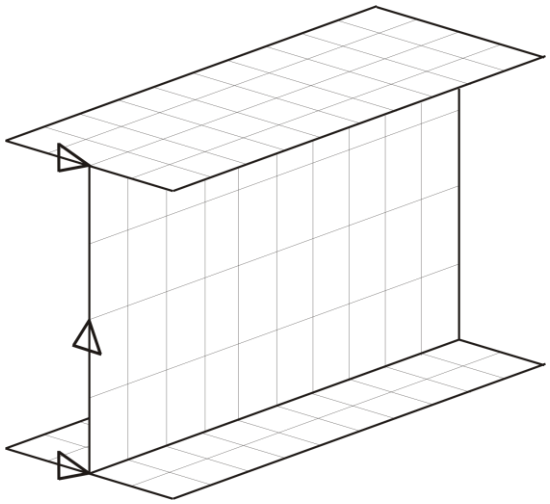

Figure 4: Discretization and end restraint in the cFEM model studies

Using the above-described shape functions, the total potential energy function can be established, from which the critical load multiplier(s) can be determined by using the usual steps of the energy method. When establishing the potential function, two options are considered here, depending on how the second-order strain term is defined. As discussed in Ádány (2012) classical buckling solutions are based on beam-theory and the assumed second-order strains are different from that applied in typical shell-theory-based numerical models (such as FSM or shell FEM). The corresponding formulae (for the longitudinal normal strain) are:

$$\varepsilon_y{}^{II,b} = \frac{1}{2}\left[\left(\frac{\partial u}{\partial y}\right)^2 + \left(\frac{\partial w}{\partial y}\right)^2\right] \text{ or } \varepsilon_y{}^{II,s} = \frac{1}{2}\left[\left(\frac{\partial u}{\partial y}\right)^2 + \left(\frac{\partial v}{\partial y}\right)^2 + \left(\frac{\partial w}{\partial y}\right)^2\right] \quad (19)$$

In the numerical examples both options are used, referred as cFEM-b and cFEM-s respectively.

Analytical formulae

Shell-model-based analytical formulae are also considered, as derived and discussed in Ádány (2012) and Ádány and Visy (2012). Formulae for critical forces can be derived by using 'beam' or 'shell' second-order strains, see Eq. (19). In case of flexural buckling the corresponding formulae are as follows:

$$F_{cr,F}{}^{b} = \frac{\pi^2 EI}{(1-\nu^2)L^2} \text{ and } F_{cr,F}{}^{s} = \frac{1}{1-\nu^2}\frac{\pi^2 EAI}{L^2 A + \pi^2 I_r} \quad (20)$$

where L is the buckling length, A is the cross-section area, I is the second moment of area to the relevant (i.e., minor or major) axis with considering the own plate inertia terms(i.e., the $bt^3/12$ terms), I_r is the second moment of area to the relevant axis with neglecting the own plate inertia terms.

$$F_{cr,T}{}^{b} = \frac{1}{r_{0S,r}{}^2}\left(\frac{\pi^2 EI_w}{(1-\nu^2)L^2} + GI_t\right) \text{ and } F_{cr,T}{}^{s} = \frac{\dfrac{\pi^2 EI_w}{(1-\nu^2)L^2} + GI_t}{r_{0S,r}{}^2 + \dfrac{\pi^2 EI_{w,r}}{EAL^2}} \quad (21)$$

where I_w and $I_{w,r}$ are warping constant, with and without considering the through-thickness warping variation, respectively, I_t is the torsion constant, while $r_{0S,r}$ is the polar radius of gyration to the shear center (calculated with neglecting the own plate inertias).

Ansys shell FE analysis
In case of shell finite element analysis the Ansys software is used (Ansys 2011). Thin shell elements are applied based on Kirchhoff plate theory (called SHELL63 in Ansys). A fine mesh is used for the FE analysis with approx. 10 000 shell elements, properly restrained to model the simple-supported ends.
The column is loaded by two concentrated longitudinal forces at its ends, equal in magnitude but opposite in direction, which is resulted a constant compression force along the column. The end forces are applied as distributed loads along the mid-lines of end cross-sections.

The analysed members are constrained in order to exclude other than global buckling modes. Three types of constraints might be necessary, as follows: (c1) constraints to exclude cross-section deformations, (c2) constraints to enforce that the cross-section planes remain planes during axial and flexural deformations, and (c3) constraints to ensure that normals to the undeformed middle line remain straight and normal during the deformations. If c1+c2+c3 (i.e. all the three) constraints are used, this leads to classical shear-free bending deformations. The practical realization of the constraints is not an obvious process. The following ways are found to be the most convenient ones.

Criterion c1 is enforced by introducing 'virtual diaphragms'. Virtual diaphragm ensures that transverse displacements (i.e., transverse translations and rotation about the column's longitudinal axis) in a cross-section are linked to each other. (In Ansys this kind of constraint can readily be realized by the CERIG command.) Criteria c2+c3 mean the exclusion of in-plane (membrane) shear deformations of the plate elements of the cross-section. A straightforward way to realize it in an Ansys FE analysis is to apply shear panels with a high value of sheta modulus (in Ansys SHELL28 are applicable). Note, some more details on how to do the constraining in Ansys can be found in Ádány and Visy (2012).

cFSM and GBT analysis
For constrained finite strip analysis the CUFSM (2006) software is applied, while the GBT analysis is performed by the GBTUL (2008) software.

Numerical results: members with uniform loading

First simple column and beam problems are shown, with uniform compressive force or uniform (major-axis) bending moment. The calculated critical forces/moments are compared in Tables 1 to 3. The tables prove that the proposed cFEM is able to reproduce the results of other methods with great precision and for a wide range of cross-sections and lengths.

Table 1 Columns with uniform compression: comparison of beam-type models

cross-section	mate-rial	buckl. type	member length	analytic	GBTUL	cFEM-b
			mm	kN	kN	kN
IPE400	Mat0	F min	1000	27239	27239	27240
IPE400	Mat0	F min	2000	6809.8	6809.8	6809.9
IPE400	Mat0	F min	5000	1089.6	1089.6	1089.6
I-narrow	Mat0	F maj	1000	211204	211204	211207
I-narrow	Mat0	F maj	2000	52801	52801	52802
I-narrow	Mat0	F maj	5000	8448.2	8448.2	8448.3
I-narrow	Mat0	T	1000	2757.8	2757.8	2757.8
I-narrow	Mat0	T	2000	1375.4	1375.4	1375.4
I-narrow	Mat0	T	5000	988.37	988.37	988.38

Table 2 Columns with uniform compression: comparison of shell-type models

cross-section	mate-rial	buckl. type	member length	analytic	cFSM	Ansys	cFEM-s
			mm	kN	kN	kN	kN
IPE400	Mat0	F min	1000	26815	26815	26825	26815
IPE400	Mat0	F min	2000	6783.0	6783.1	6784.3	6783.1
I-narrow	Mat0	F maj	1000	175509	175509	175509	175511
I-narrow	Mat0	F maj	2000	50246	50246	50252	50247
I-narrow	Mat0	T	1000	2752.9	2752.9	2753.3	2753.0
I-narrow	Mat0	T	2000	1374.8	1374.8	1374.9	1374.8

Table 3 Beams with uniform moment: comparison of various models

cross-section	mate-rial	buckl. type	member length	GBTUL	cFEM-b	cFSM	cFEM-s
			mm	kNm	kNm	kNm	kNm
IPE400	Mat0	LT	1000	5365.6	5365.7	5251.7	5251.8
IPE400	Mat0	LT	2000	1414.8	1414.9	1407.2	1407.1
IPE400	Mat0	LT	5000	295.83	295.84	295.58	295.58
I-narrow	Mat1	LT	1000	235.33	235.33	234.92	234.92
I-narrow	Mat1	LT	2000	79.561	79.561	79.526	79.526
I-narrow	Mat1	LT	5000	26.002	26.002	26.000	26.001

Numerical results: beams with non-uniform loading

For the buckling analysis an initial stress state is essential, since the potential associated with the external loading is dependent on the assumed stresses. (In other words, the geometric stiffness matrix is dependent on the stress distribution.) In the previous examples it was reasonable to assume that the only non-zero stress component is the longitudinal normal stress (σ_y), the distribution of which is either uniform or linearly changing over the cross-section. When the loading is non uniform along the length of the member, the initial stress state is less obvious.

In the following examples the cFEM buckling analysis is performed in two basic options, as far as initial stress state is considered. In option 'simple' σ_x is neglected, σ_y is defined by a simple beam-theory-based hand calculation, while τ_{xy} is assumed to be zero in the flanges while equal to the shear force per web area in the web. In case of option 'unconstrained' the initial stress state is defined by a first-order stress analysis by using the same (but unconstrained) shell model that used for the buckling analysis. Moreover, the buckling problem is solved with considering/neglecting certain stress components.

In Table 4 the effect of considered stress components is illustrated. It is obvious from the results that the in-plane shear is non-negligible. For the given problem the transverse normal stress has little effect, but this is mostly due to the fact that the assumed Poisson's ratio is zero. Finally, it is also found that for the given problem it is almost indifferent how the longitudinal stresses are calculated: by a simple beam theory or by a shell FEM analysis. It is to note, however, that in more complicated cases there might be no obvious way to calculate longitudinal stresses by a beam theory (e.g., members with holes, and/or with unusual end or intermediate restraints, etc.).

In Tables 5 and 6 the results of the cFEM analysis are compared to other methods. As it can be observed, the proposed cFEM results show excellent agreement with other methods' results.

Table 4 The effect of initial stress state

cross-section	mate-rial	buckl. type	member length	cFEM-s σ_y unconstr.	cFEM-s $\sigma_y+\tau_{xy}$ unconstr.	cFEM-s $\sigma_y+\tau_{xy}$ simple	cFEM-s $\sigma_x+\sigma_y+\tau_{xy}$ unconstr.
			mm	kNm	kNm	kNm	kNm
I-narrow	Mat1	LT	1000	736.40	320.67	320.81	320.34
I-narrow	Mat1	LT	2000	243.61	108.32	108.33	108.30

Table 5 Beams with mid-point force: comparison of beam-type models

cross-section	mate-rial	buckl. type	member length	GBTUL	cFEM-b $\sigma_y+\tau_{xy}$ simple	cFEM-b $\sigma_y+\tau_{xy}$ unconstr.	cFEM-b $\sigma_x+\sigma_y+\tau_{xy}$ unconstr.
			mm	kNm	kNm	kNm	kNm
I-narrow	Mat1	LT	1000	320.85	320.81	321.25	321.25
I-narrow	Mat1	LT	2000	108.35	108.33	108.37	108.35

Table 6 Beams with mid-point force: comparison of shell-type models

cross-section	mate-rial	buckl. type	member length	Ansys shell	cFEM-s $\sigma_y+\tau_{xy}$ simple	cFEM-s $\sigma_y+\tau_{xy}$ unconstr.	cFEM-s $\sigma_x+\sigma_y+\tau_{xy}$ unconstr.
			mm	kNm	kNm	kNm	kNm
I-narrow	Mat1	LT	1000	317.11	320.23	320.67	320.34
I-narrow	Mat1	LT	2000	108.07	108.28	108.32	108.30

Numerical results: members with holes

The previously presented examples can be solved by other numerical methods with modal feature, namely: CUFSM and/or GBTUL. To show the potential of the proposed cFEM, members with holes are also solved. If holes are present, neither GBT nor cFSM can solve the problem. At the same time, holes do not mean any difficulty or complication for the proposed cFEM at least if the member can still be modelled by using a highly regular finite element mesh. Here, two rectangular openings are assumed, as shown in Fig 5. The critical forces and moments are summarized in Tables 7 and 8.

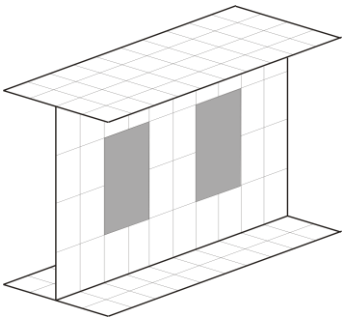

Figure 5: Members with holes

It can be concluded from the tables that the presence of holes leas to some reduction of the critical load. The reduction is dependent on the type of buckling: the most sensitive among the analyzed cases is the pure torsional buckling. Moreover, the assumed initial stress state might have non-negligible effect even if the member is subjected to pure compression. It is to observe that Ansys shell analysis results are closest to the cFEM results if 'simple' option is used, since the Ansys model itself is highly constrained, therefore its stress state is more similar to the 'simple' than to ''unconstrained' stress state of cFEM.

Table 7 Columns with holes: uniform loading

cross-section	mate-rial	buckl. type	member length	Ansys shell	cFEM-s $\sigma_y+\tau_{xy}$ simple	cFEM-s $\sigma_y+\tau_{xy}$ unconstr.	cFEM-s $\sigma_x+\sigma_y+\tau_{xy}$ unconstr.
			mm	kN/kNm	kN/kNm	kN/kNm	kN/kNm
I-narrow	Mat0	F min	1000	1037.2	1037.4	1037.6	1037.4
I-narrow	Mat0	F min	2000	259.60	259.60	259.60	259.59
I-narrow	Mat0	F maj	1000	163729	163959	166517	162596
I-narrow	Mat0	F maj	2000	48332	48342	48477	48204
I-narrow	Mat0	T	1000	2377.6	2385.2	1947.7	2199.0
I-narrow	Mat0	T	2000	1152.1	1154.3	963.05	1056.3

Table 8: The effect of holes: columns (Load1) and beams (Load3)

cross-section	mate-rial	buckl. type	member length	cFEM-s $\sigma_y+\tau_{xy}$ simple	cFEM-s $\sigma_y+\tau_{xy}$ unconstr.	cFEM-s $\sigma_x+\sigma_y+\tau_{xy}$ unconstr.
				no hole	hole	hole
			mm	kN/kNm	kN/kNm	kN/kNm
I-narrow	Mat0	F min	1000	1048.7	1037.6	1037.4
I-narrow	Mat0	F min	2000	262.38	259.60	259.59
I-narrow	Mat0	F maj	1000	175511	166517	162596
I-narrow	Mat0	F maj	2000	50247	48477	48204
I-narrow	Mat0	T	1000	2753.0	1947.7	2199.0
I-narrow	Mat0	T	2000	1374.8	963.05	1056.3
I-narrow	Mat1	LT	1000	320.23	316.60	315.97
I-narrow	Mat1	LT	2000	108.28	105.57	105.53
IPE400	Mat1	LT	1000	7126.9	7244.9	7110.2
IPE400	Mat1	LT	2000	1888.5	1894.1	1885.8

Concluding remarks

In this paper a new method, the constrained shell finite element method (cFEM) is briefly presented. The method can be considered as the extension of the constrained finite strip method: polynomial longitudinal shape functions are used which lead to significantly more general applicability. From practical point of view, by using the proposed novel shell element the following problems can readily be handled: various end restraint conditions, intermediate (partial) restraints, variable loading along the length, variable thickness along the length, holes. In the paper the proposed cFEM has been illustrated by various global (buckling) problems.

Acknowledgements

The presented work was conducted with the financial support the OTKA K108912 project of the Hungarian Scientific Research Fund.

References

Ádány, S., Schafer, B.W. (2008): A full modal decomposition of thin-walled, single-branched open cross-section members via the constrained finite strip method", *J of Const Steel Research*, 64 (1), pp. 12-29.

Ádány S. (2012): Global Buckling of Thin-Walled Columns: Analytical Solutions based on Shell Model, *Thin-Walled Structures*, Vol 55, pp 64-75.

Ádány S., Visy D. (2012): Global Buckling of Thin-Walled Columns: Numerical Studies, *Thin-Walled Structures*, Vol 54, pp 82-93.

ANSYS (2011). ANSYS Release 13.0, Ansys Inc., 2011.

Cheung Y.K., Tham L.G. (1997): The Finite Strip Method. CRC.

CUFSM (2006): Elastic Buckling Analysis of Thin-Walled Members by Finite Strip Analysis. CUFSM v3.12, http://www.ce.jhu.edu/bschafer/cufsm

GBTUL (2008): Buckling and Vibration Analysis of Thin-Walled Members. GBTUL 1.0β. DECivil/IST, 2008. Technical University of Lisbon (http://www.civil.ist.utl.pt/gbt)

Li, Z., Schafer B.W. (2009): Finite Strip Stability Solutions for General Boundary Conditions and the Extension of the Constrained Finite Strip Method, in *Trends in Civil and Structural Engineering Computing*. Stirlingshire, UK: Saxe-Coburg Publications.

Silvestre N., Camotim D., Silva N.F. (2011): Generalized Beam Theory revisited: from the kinematical assumptions to the deformation mode determination, *Int. J of Structural Stability and Dyn.*, 11(5), pp. 969-997.